Polymer 49 (2008) 2354–2361

Contents lists available at ScienceDirect

Polymer

journal homepage: www.elsevier.com/locate/polymer

Fabrication of fibril like aggregates by self-assembly of block copolymer mixtures via interpolymer hydrogen bonding

Junpeng Gao, Yuhan Wei, Binyao Li, Yanchun Han *

State Key Laboratory of Polymer Physics and Chemistry, Changchun Institute of Applied Chemistry, Chinese Academy of Sciences, Graduate School of the Chinese Academy of Sciences, 5625 Renmin Street, Changchun 130022, PR China

ARTICLE INFO

Article history:
Received 24 October 2007
Received in revised form 24 January 2008
Accepted 26 February 2008
Available online 8 March 2008

Keywords:
Block copolymers
Hydrogen-bonded complexes
Self-assembly

ABSTRACT

This paper describes the formation of fibril like aggregates from the self-assembly of block copolymer mixture (polystyrene-*b*-poly(4-vinylpyridine) (PS-*b*-P4VP) and polystyrene-*b*-poly(acrylic acid) (PS-*b*-PAA)) via interpolymer hydrogen bonding in nonselective solvent. The hydrogen bonding between P4VP and PAA in chloroform leads to the formation of complex. When all the pyridine units in P4VP were all hydrogen bonded to acrylic acid in PAA, the formed complex is insoluble, resulting in the formation of spherical micellar aggregates and nanorods. However, two kinds of supramolecules with insoluble or soluble complex are formed in the solution when PS-*b*-P4VP and PS-*b*-PAA are mixed with equal mole ratio. The fibril like aggregates can be formed from the self-assembly of supramolecule with soluble complex during spin-coating process. The effects of evaporation rate of solvent and solution concentrations on the formation of fibril like aggregates were investigated. The results prove that the kinetic factors play an important role in the formation of the fibril like aggregates.

1. Introduction

Block copolymers are well-known examples of self-assembling systems, which have two chemically distinct polymer blocks. The structures formed by block copolymer are generally nanoscale in size, ranging from 5 nm to 100 nm, and varies its morphology with slight changes in chemical structure and composition [1]. Recently, on the basis of the physical interactions, such as ionic interactions [2], coordination bond [3–8], and hydrogen bonding [9–13], between the repulsive blocks, hierarchical and functional materials were fabricated. Compared with the structure formed by neat block copolymer, novel structures can be fabricated by the blends of the block copolymers via noncovalent interactions. A higher hierarchy in structure formation was achieved by using hydrogen bonding between one of the blocks of diblock copolymer and low molecular chains in Ikkala's group [9,11,14,15]. Abetz et al. [12] demonstrated that the introduction of hydrogen bonding between poly(methacrylic acid) and poly(vinylpyridine) led to several superlattices based on the self-assembly of the corresponding block copolymers. Through controlling the amounts of proton donor units of poly(methacrylic acid), different morphologies can be obtained. In our group [16] the surface morphology of a polymeric supramolecular film consisting of symmetric PS-*b*-P4VP, dodecylbenzenesulfonic acid (DBSA), and 3-pentadecylphenol (PDP) was investigated by tuning the noncovalent interactions. From the results mentioned above, the polymeric supramolecular film structure is also determined by the effective weight fraction of the blocks and the low molecular chains hydrogen bonded to the corresponding block.

It is also well known that the noncovalent bonding between complementary polymers results in interpolymer complexes. So, another new method to fabricate micellar aggregates in common solvents through noncovalent hydrogen bonding or electrostatic interaction is proposed [17–25]. For example, Kataoka and coworkers have successfully investigated a series of new type of polymer micelles based on interpolymer ionic interactions [25–28]. In recent years, Jiang and Chen developed a series of new pathway to fabricate micelles and hollow spheres via intermolecular specific interactions [29]. Compared with micellization of amphiphilic diblock copolymers in block selective solvents, this method is more facile by just simply mixing the two components in their common solvent. Obviously, taking advantages of such strong secondary interactions, one may greatly enhance the ability toward manipulating novel and well-defined structures in a nanometer scale and explore considerable potentials amenable to practical applications. The general idea of the approach is that the intermolecular complexation can be changed significantly in terms of the polymer solubility and conformation. Core–shell micelle-like structure can be induced with the complex as the core and the remaining soluble block as the shell, which facilitates the intercomplex

* Corresponding author. Tel.: +86 431 85262175; fax: +86 431 85262126.
E-mail address: ychan@ciac.jl.cn (Y. Han).

0032-3861/$ – see front matter © 2008 Elsevier Ltd. All rights reserved.
doi:10.1016/j.polymer.2008.02.051

aggregation. All the aggregates formed in solution by this method were nearly formed as spherical micellar aggregates and vesicles when a stoichiometric ratio between the complexing blocks was used, and only few papers reported on the fabrication of other morphologies, such as wormlike aggregates [30].

At the same time, the relative lengths of different blocks have a big effect on the formation of the micellar aggregate [31]. Nonaggregating soluble complexes can be formed in the solution if the interacting blocks are sufficiently small [31]. The objects formed could thus be unimers, nonaggregating (soluble) complexes, or micelles with a swollen core, which was observed in previous reports [29,31–36]. However, to our knowledge, there are few reports on the nanostructure formations under the controlling by kinetics during the evaporation process of solvent when the soluble complexes were formed. Therefore, for this study, we have chosen to work at slight difference of solubility among the components and to vary the length of the interacting blocks as well as the evaporation rate of solvent in order to understand the influence of these parameters on the morphology of formed structures. On the other hand, it would be much more interesting to control the morphologies of the aggregates to meet the potential practical applications.

Herein, we report the formation of fibril like aggregates from the self-assembly of block copolymer mixtures (polystyrene-*b*-poly(4-vinylpyridine) (PS-*b*-P4VP) and polystyrene-*b*-poly(acrylic acid) (PS-*b*-PAA)) via interpolymer hydrogen bonding. The self-assembly is driven by the hydrogen-bonding complexation between the complementary binding sites on P4VP and PAA controlled by kinetics during the evaporation process of solvent. Different from the spherical micellar aggregates formed in solution, fibril like aggregates were observed. We found that the morphologies of the fibril like aggregates depend on the concentration of the spreading solution and the evaporation rate of solvent, indicating that kinetic factors must be playing an important role in the formation of the fibril like aggregates. The possible formation mechanisms of the structures are discussed in detail.

2. Experimental section

2.1. Materials

The diblock copolymers, polystyrene-*b*-poly(4-vinylpyridine) (PS-*b*-P4VP) and polystyrene-*b*-poly(acrylic acid) (PS-*b*-PAA), were supplied by Polymer Source, Inc., and used as-received. The number-averaged molecular weights of each block in the block copolymers are shown in Table 1. Chloroform (AR grade) was supplied by Beijing Chemical Reagent Co, and used without purification. Deionized (DI) water was obtained using the Millipore water purification system. All the glasswares were washed with the solution containing H_2SO_4 and K_2CrO_4 by sonication for 10 min in a normal ultrasonic bath (50 Hz) and were rinsed thoroughly with DI water. The silicon substrates with a 2 nm thick layer of native SiO_x were cleaned by immersion in piranha solution (3:1 concentrated H_2SO_4/H_2O_2) and sonication for 30 min. Subsequently, the substrates were rinsed repeatedly with DI water and blow dried in a N_2 flow.

Table 1
The number-averaged molecular weights (M_w) of each block in the block copolymers of PS-*b*-P4VP (PS_{307}-*b*-$P4VP_{126}$, PS_{206}-*b*-$P4VP_{198}$, PS_{32}-*b*-$P4VP_{178}$) and PS-*b*-PAA

	M_w (PS)	M_w (P4VP)
PS_{307}-*b*-$P4VP_{126}$	31 900	13 200
PS_{206}-*b*-$P4VP_{198}$	21 400	20 700
PS_{32}-*b*-$P4VP_{178}$	3300	18 700
	M_w (PS)	M_w (PAA)
PS-*b*-PAA	16 500	4500

2.2. Sample preparation

The solutions containing the two block copolymers were prepared by mixing PS-*b*-P4VP and PS-*b*-PAA in chloroform with a desired concentration and stirred for 72 h by a magnetic stirrer at room temperature. The samples were prepared by spin-coating or casting the solutions onto the freshly cleaned silicon wafers. The spin-coating speed was kept at 3000 rpm for all samples using a commercial spin-coater KW-4A, Chemat Technology Inc. All the samples were finally dried at room temperature in a vacuum for 48 h to remove any residual solvent.

2.3. Characterization

To confirm the hydrogen bonding between the P4VP and PAA blocks, Fourier transform infrared (FT-IR) spectra were taken in a Bruker evacuable IFS 66v/S (liquid nitrogen cooled MCT detector) spectrophotometer. The spectrum was collected at a resolution of 4 cm^{-1}, and 120 scans were coded to achieve the desired signal-to-noise ratio. The samples were prepared on the silicon wafer and kept under vacuum ($\approx$5 mTorr) during the process of collecting spectral data. The morphologies of the obtained products were investigated by atomic force microscopy (AFM). AFM was performed on a commercial scanning probe microscopy (SPA 300HV with an SPI 3800N probe station, Seiko Instruments Inc., Japan) in tapping mode. A silicon microcantilever (spring constant 2 N/m and resonance frequency 70 kHz, Olympus, Japan) with an etched conical tip (radius of curvature is 40 nm as characterized by scanning over very sharp needle array, NT-MDT, Russia) was used for scan. Dynamic light scattering (DLS) was performed with a spectrometer (DAWN EOS and QELS, Waytt Technology Corporation, America). All measurements were carried out at 15 °C, with a detection angle of 90°.

3. Results and discussion

In this section, we start by the characterization of the formation of supramolecular complex. Then we investigate various aggregate formations prepared by spin-coating or casting the chloroform solutions containing PS-*b*-P4VP and PS-*b*-PAA with different mole ratios and concentrations onto the silicon wafers. Subsequently, we give a possible mechanism for the formation of fibril like aggregates.

3.1. Formation of supramolecular complex

It is well known that PAA is a polyacid and P4VP is a polybase. Hydrogen bonding should occur between pyridine and acrylic acid. When the concentration of PS-*b*-PAA was fixed at 0.042 wt%, while the concentrations of PS_{307}-*b*-$P4VP_{126}$, PS_{206}-*b*-$P4VP_{198}$, and PS_{32}-*b*-$P4VP_{178}$ were 0.044 wt%, 0.028 wt%, 0.016 wt%, respectively, all the pyridine units in P4VP were hydrogen bonded to acrylic acid in PAA, which can be verified by the FT-IR spectra shown in Fig. 1a. In FT-IR spectra (Fig. 1a), pure PS-*b*-P4VP has an adsorption peak at the band of 993 cm^{-1}, which arises from the distortion vibration of the pyridine ring. Upon complexation with acrylic acid in PAA, the distortion vibration of the pyridine ring disappeared, indicating that all the pyridine units in P4VP were hydrogen bonded to acrylic acid in PAA.

For the system of PS-*b*-P4VP (PS_{307}-*b*-$P4VP_{126}$, PS_{206}-*b*-$P4VP_{198}$, PS_{32}-*b*-$P4VP_{178}$) mixed with PS-*b*-PAA with equal mole ratio, the FT-IR spectra are shown in Fig. 1b. For the spectrum of PS-*b*-PAA, the bands near 1742 cm^{-1} and 1713 cm^{-1} correspond to the free

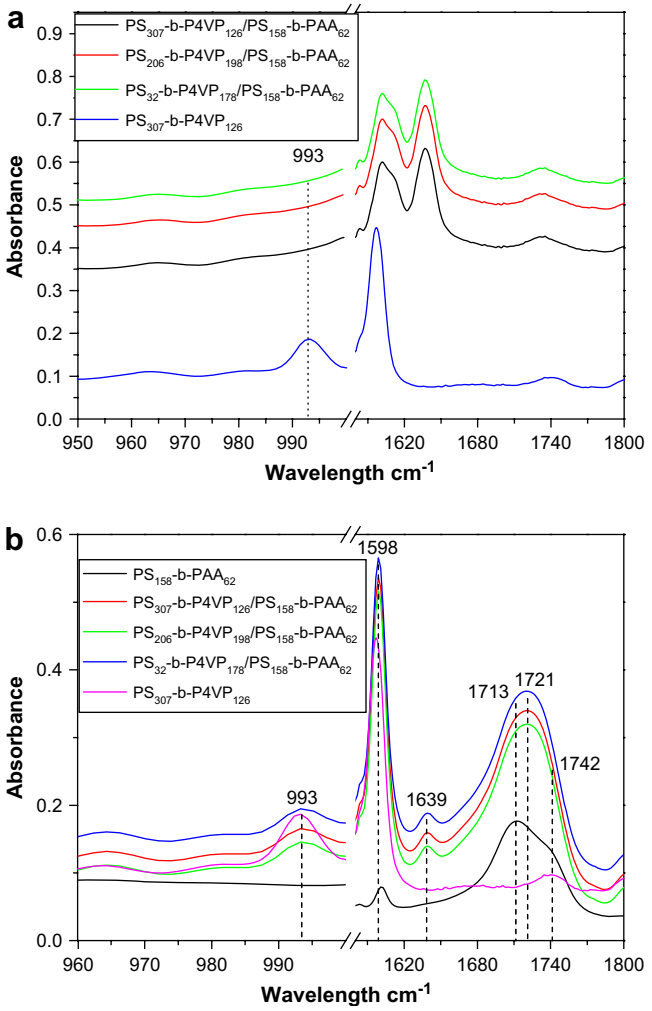

Fig. 1. FT-IR spectra of PS_{307}-*b*-$P4VP_{126}$, and the mixture of PS-*b*-P4VP (PS_{307}-*b*-$P4VP_{126}$, PS_{206}-*b*-$P4VP_{198}$, PS_{32}-*b*-$P4VP_{178}$) and PS-*b*-PAA after the complete protonation of pyridine units in P4VP by acrylic acid in PAA. (b) The mixture of PS-*b*-P4VP (PS_{307}-*b*-$P4VP_{126}$, PS_{206}-*b*-$P4VP_{198}$, PS_{32}-*b*-$P4VP_{178}$) and PS-*b*-PAA with 1:1 mole ratio. All pyridine units in P4VP were hydrogen bonded to acrylic acid in PAA.

carboxyl group and the dimer of acrylic acid unit, respectively. While in the spectra of the blend, a new band at 1721 cm^{-1} appears which is attributed to the "free" carbonyl groups formed by an interaction between the pyridine nitrogen atom and the hydroxyl group of acrylic acid. Moreover, pure PS-*b*-P4VP has an adsorption peak at 1596–1598 cm^{-1}, which arises from the aromatic carbon–carbon stretching band of the phenyl groups of the PS block and the aromatic carbon–nitrogen stretching band of the unprotonated pyridine rings within the P4VP block [37] and at 993 cm^{-1} for the distortion vibration of the pyridine ring. Upon complexation with acrylic acid in PAA, the carbon–nitrogen stretching band at 1596 cm^{-1} is expected to shift to higher wavenumbers, 1639 cm^{-1}, which corresponds to the protonated P4VP [37,38]. These results indicate that the hydrogen-bonding interaction has taken place between P4VP and PAA in the solution. However, the distortion vibration of the pyridine ring in P4VP at 993 cm^{-1} also exists, although the intensity was decreased due to the protonation by acrylic acid in PAA. This result confirmed that some free pyridine units in P4VP still existed in the solution because the number of pyridine units in P4VP was larger than that of acrylic acid in PAA. Thus, two kinds of supramolecules composed of PS-*b*-P4VP and PS-*b*-PAA via hydrogen bonding can be expected (Scheme 1). The supramolecule 1 has an insoluble complex formed by P4VP and PAA via hydrogen bonding, because nearly all the pyridine units in P4VP were

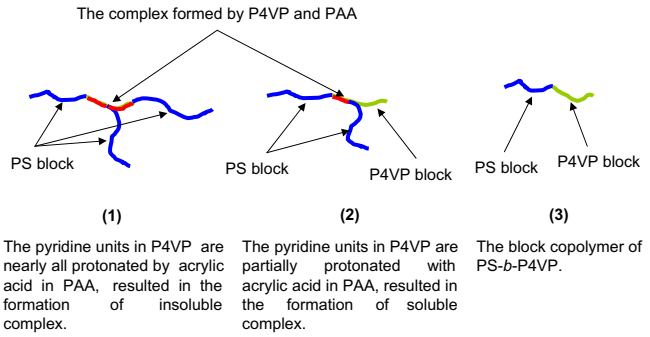

Scheme 1. The model of supramolecules composed of PS-*b*-P4VP and PS-*b*-PAA: (1) the supramolecules without free pyridine units (the pyridine units were all protonated by acrylic acid in PAA); (2) the supramolecules with some free pyridine units (the pyridine units were partially protonated by acrylic acid in PAA); (3) PS-*b*-P4VP molecules in the solution.

hydrogen bonded to acrylic acid in PAA. However, the supramolecule 2 has a soluble complex, because the formed P4VP/PAA complex is relatively small and the solvent of chloroform is good enough to solubilize it [31]. Another kind of molecules existed in solution is free PS-*b*-P4VP. Therefore, for the system of PS-*b*-P4VP (PS_{307}-*b*-$P4VP_{126}$, PS_{206}-*b*-$P4VP_{198}$, PS_{32}-*b*-$P4VP_{178}$) mixed with PS-*b*-PAA with equal mole ratio, supramolecule 1, supramolecule 2 and free PS-*b*-P4VP coexisted in the solution.

3.2. Formation of the structure of fibril like aggregates

After spin-coating the solutions containing PS-*b*-PAA and PS-*b*-P4VP (PS_{307}-*b*-$P4VP_{126}$, PS_{206}-*b*-$P4VP_{198}$ and PS_{32}-*b*-$P4VP_{178}$) all the pyridine units in P4VP that were hydrogen bonded to acrylic acid in PAA from chloroform onto the silicon wafers, short nanorods and spherical micellar aggregates (Fig. 2) were observed. The average diameter was 37 nm, 35 nm, and 28 nm, respectively. Dynamic light scattering (DLS) is the most suitable technique to characterize the aggregates in solution since it is sensitive to the existence of large complexes. Fig. 3 shows the apparent hydrodynamic radius distributions of the solution blends of PS-*b*-PAA and PS-*b*-P4VP. The diameter of most aggregates in solution was between 30 nm and 300 nm. The peaks of the hydrodynamic diameter of aggregates were broad, indicating that both the spherical micelles and the nanorods with relative long length existed in solution.

After spin-coating the solutions containing PS-*b*-PAA and PS-*b*-P4VP (PS_{307}-*b*-$P4VP_{126}$, PS_{206}-*b*-$P4VP_{198}$, PS_{32}-*b*-$P4VP_{178}$) with equal mole ratio onto the silicon wafers, some fibril like aggregates coexisting with some spherical micellar aggregates were observed at room temperature (Fig. 4a–c, the total concentration for a–c is 0.06 wt%, 0.06 wt%, and 0.04 wt%, respectively). The length of the fibril like aggregates was about 300–500 nm and the average diameter formed by PS-*b*-PAA and PS_{307}-*b*-$P4VP_{126}$ is about 40 nm, which is larger than that of the fibril like aggregates formed by PS-*b*-PAA and PS_{206}-*b*-$P4VP_{198}$ (the average diameter: 30 nm), and PS_{32}-*b*-$P4VP_{178}$ (the average diameter: 20 nm). Under this condition, the preponderant structure was spherical micellar aggregate. The average diameter of the spherical aggregates was about 26 nm, 30 nm, and 22 nm for Fig. 4a–c, respectively. To investigate the micellization behavior in solution, dynamic light scattering (DLS) was used. Fig. 5a shows the apparent hydrodynamic radius distributions of the solution blends of PS-*b*-PAA and PS-*b*-P4VP with the same concentrations as in Fig. 4a–c. The diameter of most aggregates in solution was between 60 nm and 90 nm, indicating that only spherical micellar aggregates were formed in solution. Because the spherical micelles in solution were swollen by solvent, the diameters of the spherical micelles detected by DLS were larger than that of the dry micelles on the silicon wafers.

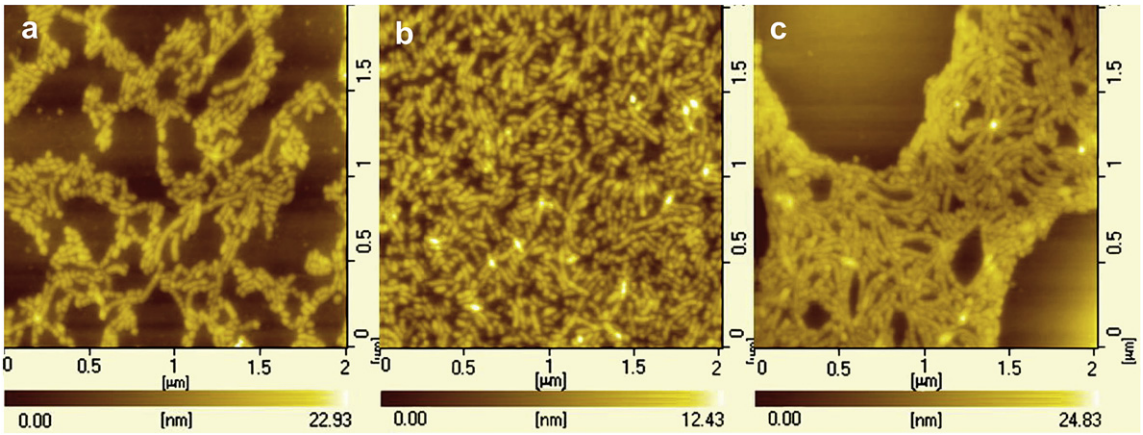

Fig. 2. Representative AFM topographic images of the spherical micellar aggregates formed on the silicon wafers when all the pyridine units in P4VP were all hydrogen bonded to acrylic acid in PAA. The concentration of PS-*b*-PAA was fixed at 0.042 wt%, while the concentrations of (a) PS_{307}-*b*-$P4VP_{126}$, (b) PS_{206}-*b*-$P4VP_{198}$, (c) PS_{32}-*b*-$P4VP_{178}$ were 0.044 wt%, 0.028 wt%, 0.016 wt%, respectively.

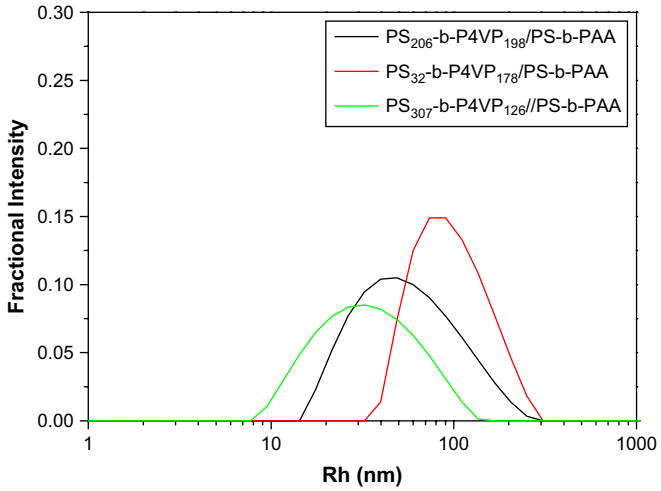

Fig. 3. The distribution of the hydrodynamic radius (R_h) from the DLS correlation functions of PS-*b*-PAA and PS-*b*-P4VP. The concentration of the solutions was the same as the concentrations in Fig. 2.

However, the fibril like aggregates with the length about 300–500 nm were not found in solution.

The effect of the polymer concentration on the morphology of the structure is shown in Fig. 4d–l. The mole ratio between PS-*b*-P4VP and PS-*b*-PAA was also fixed at 1:1. When the total polymer concentration was increased from 0.06 wt% to 0.12 wt%, from 0.06 wt% to 0.12 wt%, and from 0.04 wt% to 0.08 wt% for the system of PS-*b*-PAA and PS_{307}-*b*-$P4VP_{126}$, PS-*b*-PAA and PS_{206}-*b*-$P4VP_{198}$, and PS-*b*-PAA and PS_{32}-*b*-$P4VP_{178}$, respectively, after spin-coating the solutions onto the silicon wafers, the fibril like aggregates along with spherical micellar aggregates were also found (Fig. 4d–f). As shown in Fig. 4d–f, the average diameters of the fibril like aggregates were increased from 40 nm to 115 nm, from 30 nm to 75 nm, and from 20 nm to 65 nm, and the length was increased to several micrometers. In addition, compared with the structures formed in Fig. 4a–c, the fibril like aggregates were preponderant structures. Fig. 5b shows the apparent hydrodynamic radius distributions of the solution blends of PS-*b*-PAA and PS-*b*-P4VP with the same concentrations as in Fig. 4d–f. The diameter of most aggregates in solution was between 60 nm and 120 nm. This radius distribution indicated that the aggregates formed in solution were spherical micelles but not the fibril like aggregates (the length was about 500–2000 nm).

When the total polymer concentration of the system of PS-*b*-PAA and PS_{307}-*b*-$P4VP_{126}$, PS-*b*-PAA and PS_{206}-*b*-$P4VP_{198}$, and PS-*b*-PAA and PS_{32}-*b*-$P4VP_{178}$ was further increased to 0.21 wt%, 0.21 wt%, 0.15 wt%, respectively, the fibril like aggregates with long length were not found (Fig. 4g–i). The films were all featured as wormlike cylinders and protuberance. When the total polymer concentration was further increased (PS-*b*-PAA and PS_{307}-*b*-$P4VP_{126}$ (0.42 wt%), PS-*b*-PAA and PS_{206}-*b*-$P4VP_{198}$ (0.42 wt%), and PS-*b*-PAA and PS_{32}-*b*-$P4VP_{178}$ (0.30 wt%)), the structures of wormlike cylinders were markedly weakened (Fig. 4j–l), and a kind of featureless film with some protuberance was obtained. Because the spherical micellar aggregates were formed in solution, it is reasonable to think that the spherical protuberance on the film is expected as the spherical micellar aggregates.

The effect of evaporation rate on the formation of aggregates was also investigated. A droplet of solutions with different concentrations (the solutions used in this case were the same as that of in Fig. 4a–f) was cast onto the silicon wafer, and subsequently dried in ambient atmosphere at room temperature. When the polymer concentrations were used as the same as in Fig. 4a–c, fibril like aggregates were not found (Fig. 6a–c). Except for the existence of spherical micellar aggregates, the continuous polymer films were obtained. When the concentration of the solutions was increased and used as the same as in Fig. 4d–f, featureless continuous films were obtained (Fig. 6d–f).

3.3. Formation mechanism of the fibril like aggregates

From the above experimental results, spherical micellar aggregates and nanorods were formed by the supramolecules with insoluble complex when all the pyridine units were hydrogen bonded to acrylic acid. If PS-*b*-P4VP mixed with PS-*b*-PAA with equal mole ratio, not all the pyridine units were hydrogen bonded to acrylic acid, and two kinds of supramolecules and free PS-*b*-P4VP were obtained. Fibril like aggregates coexisting with spherical micellar aggregates could be obtained after spin-coating the solutions containing the two block copolymers with equal mole ratio with low concentrations. With increasing the concentration to a certain level, fibril like aggregates disappeared and only spherical micellar aggregates could be obtained. Compared with the condition with fast evaporation of solvent, fibril like aggregates also could not be formed when the evaporation was slow. According to the above results and analysis, a mechanism can be suggested for the formation of fibril like aggregates. Two factors are crucial for the formation of structures: the solubility of the complex formed by PAA and P4VP and the kinetic factor.

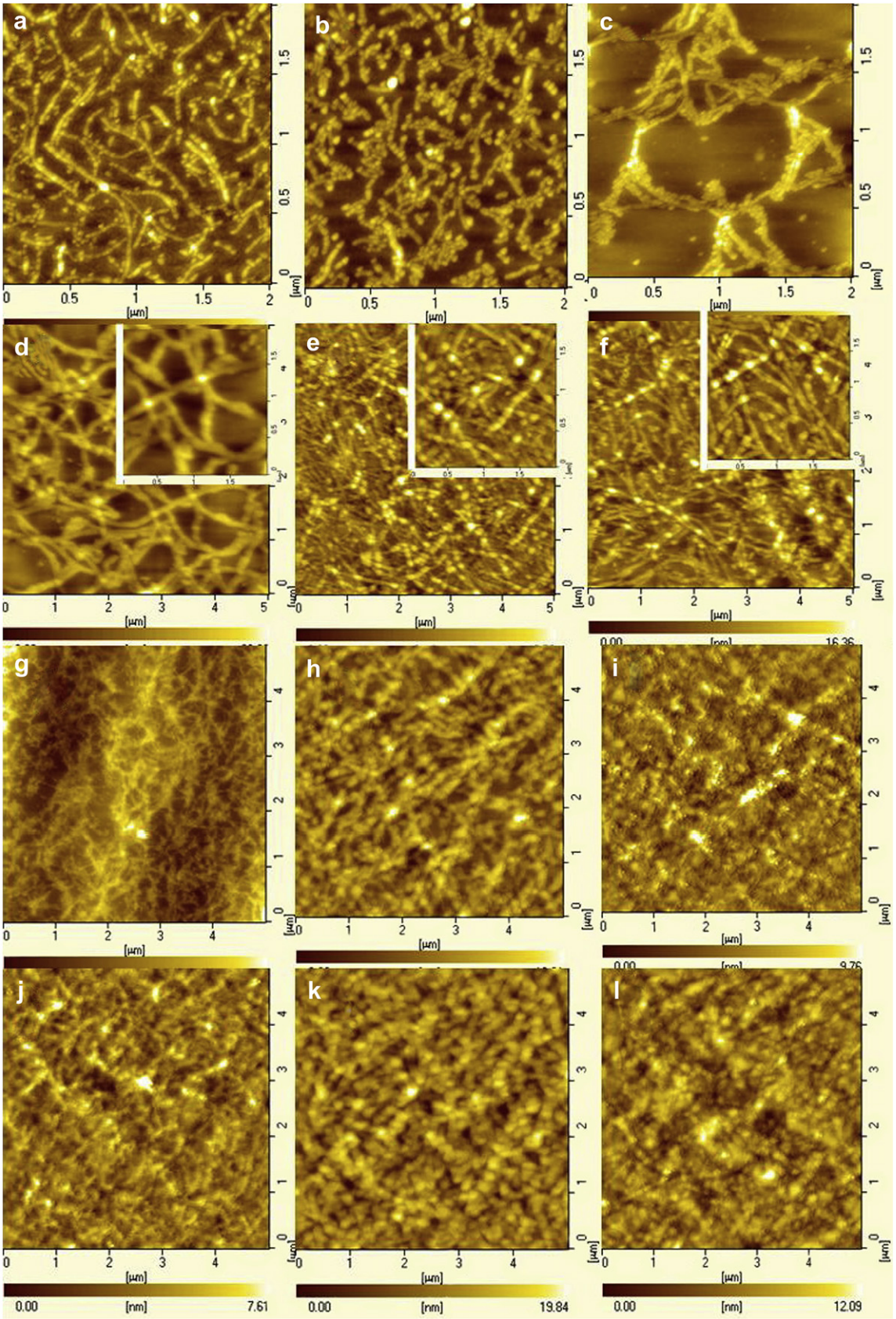

Fig. 4. Representative AFM topographic images of structures formed on the silicon wafers after spin-coating the solutions with different concentrations. PS-*b*-PAA and PS_{307}-*b*-$P4VP_{126}$ ((a) 0.06 wt%, (d) 0.12 wt%, (g) 0.21 wt%, (j) 0.42 wt%), PS-*b*-PAA and PS_{206}-*b*-$P4VP_{198}$ ((b) 0.06 wt%, (e) 0.12 wt%, (h) 0.21 wt%, (k) 0.42 wt%), and PS-*b*-PAA and PS_{32}-*b*-$P4VP_{178}$ ((c) 0.04 wt%, (f) 0.08 wt%, (i) 0.14 wt%, (l) 0.30 wt%). The mole ratio of the two block copolymers was fixed at 1:1.

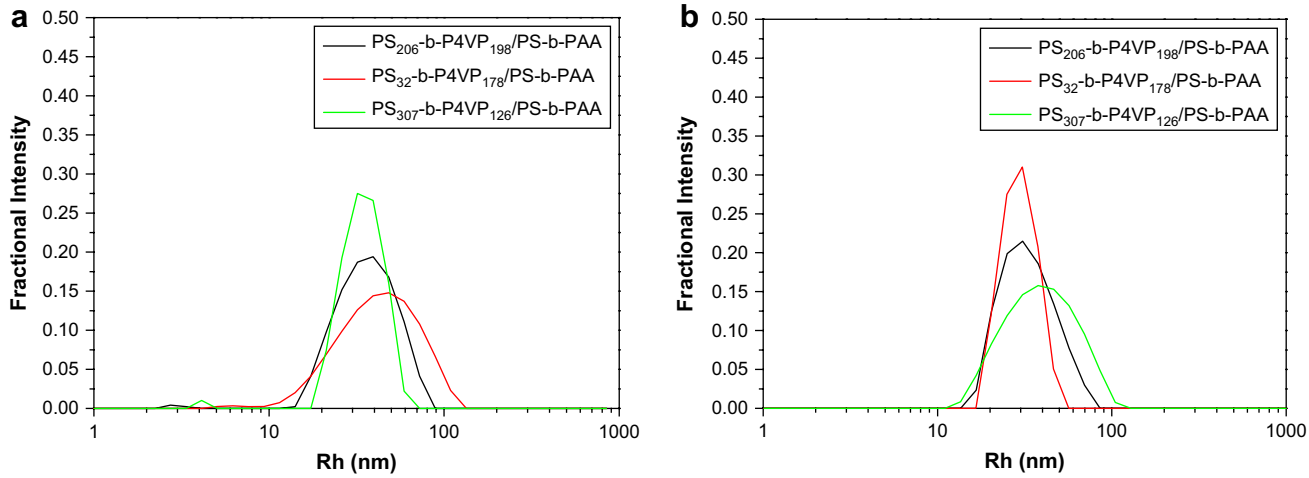

Fig. 5. The distribution of the hydrodynamic radius (R_h) from the DLS correlation functions of PS-*b*-PAA and PS-*b*-P4VP (PS_{307}-*b*-$P4VP_{126}$, PS_{206}-*b*-$P4VP_{198}$, PS_{32}-*b*-$P4VP_{178}$). The concentration of the solutions was the same as the concentrations in Fig. 4a–c (a) and d–f (b).

Just like the spherical micellar aggregates' formation mechanism in previous literatures [17–25], spherical micellar aggregates with insoluble core formed by P4VP and PAA via hydrogen bonding and PS corona were formed when the insoluble complex was formed. In this case, when all the pyridine units in P4VP were hydrogen bonded to acrylic acid in PAA, only the kind of supramolecule 1 with insoluble complexes was formed. Thus, the spherical micellar aggregates and nanorods that composed of a hydrogen-bonded PAA/P4VP core and a soluble PS corona were formed. It is well known that the formed micellar aggregates in solution had not enough time to restructure itself during the drying process, because the spin-coating process is fast. So the fibril like aggregates could not be formed by restructuring the micelles or nanorods during the spin-coating process.

For the system containing supramolecule 1, supramolecule 2 and free PS-*b*-P4VP, both spherical micellar aggregates and fibril like aggregates were formed after spin-coating the solutions onto the silicon wafers. Since the fibril like aggregates were not formed both in solution and by the restructuring of the spherical micellar aggregates during the spin-coating process, it is reasonable that

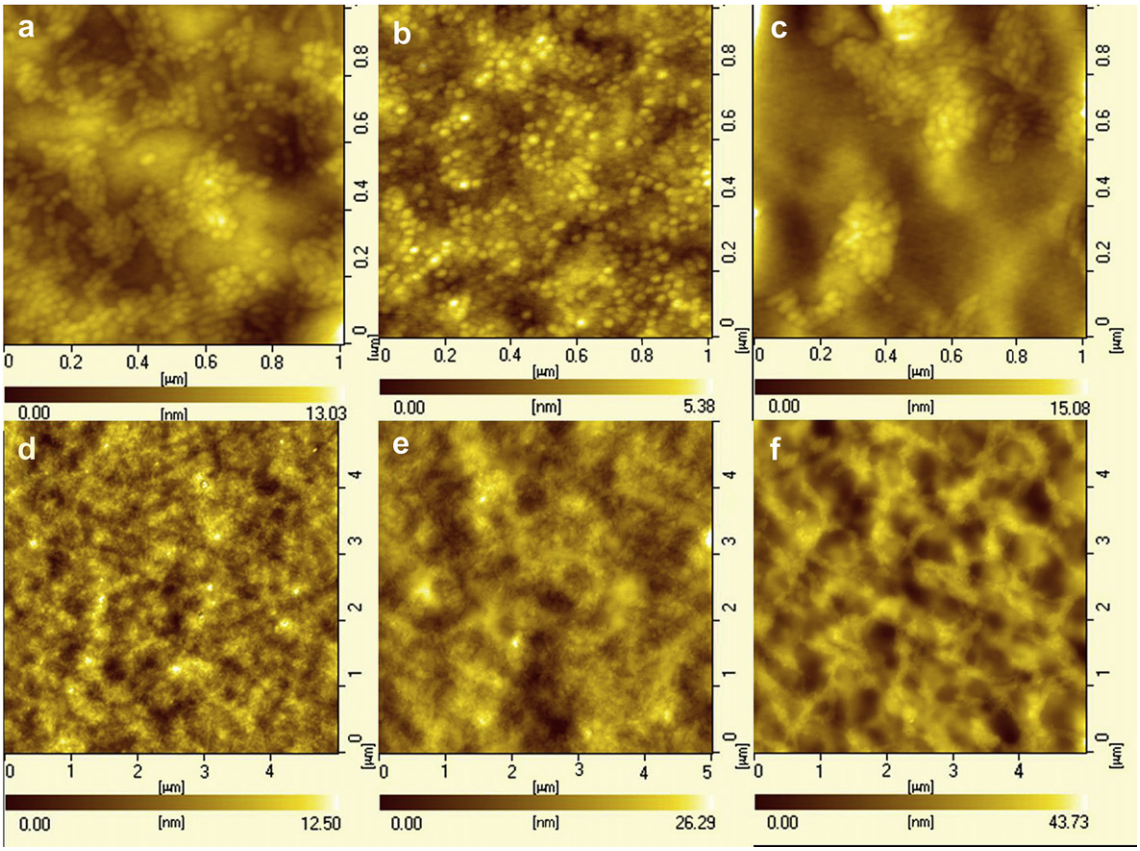

Fig. 6. Representative AFM topographic images of the spherical micellar aggregates and continuous films by casting the solutions containing PS-*b*-PAA and PS_{307}-*b*-$P4VP_{126}$ ((a) 0.06 wt%, (d) 0.12 wt%), PS-*b*-PAA and PS_{206}-*b*-$P4VP_{198}$ ((b) 0.06 wt%, (e) 0.12 wt%), and PS-*b*-PAA and PS_{32}-*b*-$P4VP_{178}$ ((c) 0.08 wt%, (f) 0.04 wt%) on the silicon wafers. The mole ratio of the two block copolymers was fixed at 1:1.

the fibril like aggregates were formed by the self-assembly of supramolecule with soluble complex (supramolecule 2, Scheme 1) during the spin-coating process. Although the complex formed by P4VP and PAA in supramolecule 2 is soluble in chloroform, PS and P4VP have a better solubility than that. In our opinion, the kinetic factors attributed to the solvent have a preferential affinity for the component of PS and free P4VP in the supramolecule 2, because the complex of P4VP/PAA has a lower solubility. As we know, the evaporation of solvent during spin-coating is very fast. Under the condition of fast evaporation, kinetic arrest in the polymer might have taken place before the chains had enough time to make the rearrangements needed to obtain any equilibrium morphology occurred in the course of the evaporation [39]. Therefore, the complex of P4VP/PAA could solidify first during the process of spin-coating. The phase separation between PS and P4VP took place at the same time, resulting in the formation of aggregates with P4VP/PAA core and free P4VP and PS corona. During the process of self-assembly, the free P4VP chain offered the chance for linking the two aggregates together, resulting in the formation of fibril like aggregates (Fig. 4a–f).

At low concentrations (Fig. 4a–c), the number of the complexes formed by P4VP and PAA is also small, so the linking chance between two aggregates is small. Thus, the fibril like aggregates were relatively short. With increasing the polymer concentration (Fig. 4d–f), the chance of link between the two aggregates may be increased, and the length of the fibril like aggregates will be increased from several nanometers to several micrometers. This is the reason why the preponderant structure in Fig. 4a–c is the spherical micellar aggregates, while the fibril like aggregates with long length are dominant in Fig. 4d–f. As known, with increasing the concentration of polymer in a given solvent, the solvent–polymer interaction will decrease while the polymer–polymer interaction will increase. Thus, when the concentration was further increased to a certain level (Fig. 4g–l), the slight difference of solubility between the complex of P4VP/PAA and PS, P4VP was weakened during the spin-coating process, resulting in the weak self-assembly tendency of the supramolecule 2. Thus, the fibril like aggregates cannot be formed during the spin-coating process, but the featureless film. This phenomenon is similar to the results obtained by Moffitt and Baker [40–42].

When a droplet of solutions with different concentrations (the solutions used in this case were the same as that of in Fig. 4a–f) was cast onto the silicon substrate and subsequently dried at ambient atmosphere at room temperature, the speed of solvent evaporation is much slower than that of process of spin-coating. Under the condition of slow evaporation speed, the absence of fibril like aggregates proved that the formation was controlled by kinetics during the spin-coating process. With slow evaporation, the solution is gradually concentrated, and the slight difference of solubility among the complex of P4VP/PAA, free P4VP and PS is not obvious because the polymer chain has enough time to make rearrangements needed to obtain any equilibrium morphology [40]. Thus, the self-assembly trend of the supramolecule 2 was weakened, and fibril like aggregates were not formed. Because the spherical micellar aggregates were formed by the supramolecule 1 with insoluble complex in solution, the spherical micellar aggregates were also observed on the surface. For the increased concentrations, the enough movement of polymer chains led to the formation of continuous films, and the spherical micellar aggregates may be embedded in the film after the evaporation of solvent (Fig. 6d–f).

As discussed above, the supramolecule 1 has an insoluble complex and can self-assemble into spherical micellar aggregates in solution. The supramolecule 2 has a soluble complex and the objects formed in solution could thus be unimers, nonaggregating (soluble) complexes [31]. During the process of fast evaporation of solvent, the difference among the components is obvious, and the supramolecule 2 can self-assemble into fibril like aggregates controlled by kinetics when the concentration of the solution is low. Under the condition of slow evaporation of solvent, the polymer chains have enough time to move to obtain equilibrium state, and the difference among the components is not obvious. Thus, the fibril like aggregates cannot be formed. These results indicate that two factors are crucial for the formation of structures: the solubility of the complex formed by PAA and P4VP and the kinetic factor.

4. Conclusions

The fibril like aggregates have been fabricated from the self-assembly of block copolymer mixture (polystyrene-*b*-poly(4-vinylpyridine) (PS-*b*-P4VP) and polystyrene-*b*-poly(acrylic acid) (PS-*b*-PAA)) via hydrogen bonding. Spherical micellar aggregates are formed by the supramolecules with insoluble complexes in solution. The kind of supramolecules with a soluble complex can self-assemble into fibril like aggregates by controlling the solvent evaporation rate and solution concentration. The formation of the fibril like aggregates is controlled by the solubility of the complex formed by PAA and P4VP and kinetic factor.

Acknowledgments

This work was subsidized by the National Natural Science Foundation of China (20621401, 50573077, 50773080) and the Ministry of Science and Technology of China (2003CB615601).

References

[1] Bates FS, Fredrickson GH. Annu Rev Phys Chem 1990;41:525.
[2] Horvat A, Lyakhova KS, Sevink JA, Zvelindovsky AV, Magerle R. J Chem Phys 2004;120:1117.
[3] Antonietti M, Conrad J, Thunemann A. Macromolecules 1994;27:6007.
[4] Ruokolainen J, Tanner J, Brinke G, Ikkala O, Torkkeli M. Macromolecules 1995;28:7779.
[5] Al-Hussein M, Lohmeijer BGG, Schubert US, Jeu WH. Macromolecules 2003;36:9281.
[6] Ooe M, Murata M, Mizugaki T, Ebitani K, Kaneda K. J Am Chem Soc 2004;126:1604.
[7] Gao J, Fu J, Lin C, Lin J, Han Y, Yu X, et al. Langmuir 2004;20:9775.
[8] Tang M, Dou H, Sun K. Polymer 2006;47:728.
[9] Ruokolainen J, Tanner J, Ikkala O, Brinke G, Thomas EL. Macromolecules 1998;31:3532.
[10] Manna S, Nandi AK. J Phys Chem B 2004;108:6932.
[11] van Ekenstein GA, Nijand EPH, Ikkala O, Brinke G. Macromolecules 2003;36:3684.
[12] Jiang S, Gopfent A, Abetz V. Macromolecules 2003;36:6171.
[13] Gao L, Shi L, An Y, Zhang W, Shen X, Guo S, et al. Langmuir 2004;20:4787.
[14] Ruokolainen J, Brink G, Ikkala O. Adv Mater 1999;11:777.
[15] Ruokolainen J, Mäkinen R, Torkkeli M, Mäkelä T, Serimaa R, ten Brinke G, et al. Science 1998;280:557.
[16] Zhang P, Gao J, Li B, Han Y. Macromol Rapid Commun 2006;27:295.
[17] Gao W, Bai Y, Chen E, Li Z, Han B, Yang W, et al. Macromolecules 2006;39:4894.
[18] Zhang W, Shi L, Gao L, An Y, Li G, Wu K, et al. Macromolecules 2005;38:899.
[19] Liu S, Zhu H, Zhao H, Jiang M, Wu C. Langmuir 2000;16:3712.
[20] Topouza D, Orfanou K, Pispas S. J Polym Sci Part A Polym Chem 2004;42:6230.
[21] Ilhan F, Galow TH, Gray M, Clavier G, Rotello VM. J Am Chem Soc 2000;122:5895.
[22] Laicer CST, Mrozek RA, Taton TA. Polymer 2007;48:1316.
[23] Lee LT, Woo EM, Hou SS, Förster S. Polymer 2006;47:8350.
[24] Strandman S, Hietala S, Aseyev V, Koli B, Butcher SJ, Tenhu H. Polymer 2006;47:6524.
[25] Harada A, Kataoka K. Science 1999;28:365.
[26] Harada A, Kataoka K. Macromolecules 1998;31:288.
[27] Harada A, Kataoka K. Macromolecules 1995;28:5294.
[28] Strandman S, Zarembo A, Darinskii AA, Löflund B, Butcher SJ, Tenhu H. Polymer 2008;48:7008.
[29] Cheng D, Jiang M. Acc Chem Res 2005;38:494.
[30] Xiong D, Shi L, Jiang X, An Y, Chen X, Lu J. Macromol Rapid Commun 2007;28:194.
[31] Lefevre N, Fustin CA, Varshney SK, Gohy JF. Polymer 2007;48:2306.
[32] Jiang M, Li M, Xiang M, Zhou H. Adv Polym Sci 1999;14:6121.

[33] Kabanov AV, Bronich TK, Kabanov VA, Yu K, Eisenberg A. Macromolecules 1996;29:6797.
[34] Gohy JF, Varshney SK, Antoun S, Jerome R. Macromolecules 2000;33:9298.
[35] Harada A, Kataoka K. J Controlled Release 2001;72:85.
[36] Gohy JF, Varshney SK, Jerome R. Macromolecules 2001;34:3361.
[37] Kosonen H, Valkama S, Ruokolainen J, Torkkeli M, Serimaa R, ten Brinke G, et al. Eur Phys J E 2003;10:69.
[38] Ruotsalainen T, Torkkeli M, Serimaa R, Mkelä T, Ruokolainen RJ, ten Brinke G, et al. Macromolecules 2003;36:9437.
[39] Zhang Q, Tsui OKC, Du B, Zhang F, Tang T, He T. Macromolecules 2000;33:9561.
[40] Zheng W, Angelopoulos M, Epstein AJ, MacDiarmid AG. Macromolecules 1997; 30:7634.
[41] Devereaux CA, Baker SM. Macromolecules 2002;35:1921.
[42] Cheyne RB, Moffitt MG. Langmuir 2005;21:5453.